

Technical University of Denmark



Large field SPIV with separated sheets in a spanwise plane of a turbulent boundary layer with vortex generators

Foucaut, J.M.; Coudert, S.; Braud, C.; Velte, Clara Marika

Published in:

Proceedings of the 16th International Symposium on Applications of Laser Techniques to Fluid Mechanics

Publication date:

2012

Document Version

Publisher's PDF, also known as Version of record

[Link back to DTU Orbit](#)

Citation (APA):

Foucaut, J. M., Coudert, S., Braud, C., & Velte, C. M. (2012). Large field SPIV with separated sheets in a spanwise plane of a turbulent boundary layer with vortex generators. In Proceedings of the 16th International Symposium on Applications of Laser Techniques to Fluid Mechanics

DTU Library

Technical Information Center of Denmark

General rights

Copyright and moral rights for the publications made accessible in the public portal are retained by the authors and/or other copyright owners and it is a condition of accessing publications that users recognise and abide by the legal requirements associated with these rights.

- Users may download and print one copy of any publication from the public portal for the purpose of private study or research.
- You may not further distribute the material or use it for any profit-making activity or commercial gain
- You may freely distribute the URL identifying the publication in the public portal

If you believe that this document breaches copyright please contact us providing details, and we will remove access to the work immediately and investigate your claim.

Large field SPIV with separated sheets in a spanwise plane of a turbulent boundary layer with vortex generators

J.M. Foucaut¹, S. Coudert², C. Braud², C. Velte³

1-2: Univ. Lille Nord de France F-59000 Lille, EC Lille¹, CNRS²,
Laboratoire de Mécanique de Lille (UMR 8107)

Boulevard Paul Langevin, 59655 Villeneuve d'Ascq Cedex,

3: Department of Wind Energy,

Technical University of Denmark - DTU

Nils Koppels Allé Building 403, 2800 Kgs. Lyngby, Denmark

* corresponding author: jean-marc.foucaut@ec-lille.fr

Abstract The Stereoscopic PIV is nowadays a well established measurement technique for turbulent flows. However, the accuracy and the spatial resolution are still highly questionable in presence of complex flow with both strong gradients and out of plane motions. To give guidelines for both setup and measurements of such flow configurations, a large region of overlap between two SPIV systems on the same laser light sheet is acquired in a plane normal to the streamwise direction of a high Reynolds turbulent boundary layer flow. A simple separation of the two light sheets is used to improve the accuracy of measurements by increasing the velocity dynamic range especially. It also presents the enhancement of accuracy due to the light sheets separation for characterizing streamwise vortices (i.e. perpendicular to the sheet). The present experiment was performed in the Laboratoire de Mécanique de Lille wind tunnel facility which has been specially designed to study fully developed turbulent boundary layer at high Reynolds number. The outlooks are to study in detail the physics of the streamwise vortices generated from vortex generators taking advantage of large scales of this turbulent boundary layer.

1. Introduction

The SPIV is now a reliable method to measure velocity fields in complex and turbulent flows (Adrian (1991), Westerweel (1997), Prasad (2000)). However, the accuracy is each time a new challenge when complexities are added in the flow such as strong gradients, strong out of plane motions and a large field. The difficulties increase strongly when the measurement plane is normal to the flow. In this case, the out of plane motion of the particles is induced by the main component of the flow. If the PIV delay is adjusted to obtain a minimum of isolated particles due to particles entering and getting out the light sheet, the dynamic range tends to zero and the accuracy is then very poor. A solution, discussed in the present paper, is to separate the two light sheets of a distance corresponding to the mean dynamic.

In the present work, we focus on measurements behind vortex generators embedded in a high Reynolds turbulent boundary layer where all these problems are encountered. These types of actuators are generally used in flow control to try to delay separation, reduce pressure or viscous drag found in many applications such as aeronautics, wind turbines and maritime applications (Gad-el-Hak (2000)). From the use of two PIV systems, it is possible to obtain a large zone of overlap where precision of measurements will be investigated. This study will help to give guidelines for measurements of such flow configurations. In the present paper, the experimental setup will be first presented, the accuracy will be then discussed focusing on the flow without vortex generators and finally an example of result with the actuators will be presented.

1. Experimental setup

The Laboratoire de Mécanique de Lille (LML) wind tunnel facility has been specially designed to study fully developed turbulent boundary layer at high Reynolds number. The 20 m long test section allows a boundary layer thickness of about 30 cm (Carlier and Stanislas (2005)). In this wind tunnel, an experiment was performed to characterize vortices made by specific vortex generators in the turbulent boundary layer. Two families of generators have been used for this experiment,

- passive vortex generators which behave like obstacles in the flow. The flow by-passing the obstacles creates streamwise vortices.
- inclined air jets whose interactions with the main flow also create vortices.

The large dimensions of the boundary layer allow us to study in detail the physics of the vortices with a good accuracy. A large field Stereoscopic Particle Image Velocimetry (PIV) in a plane normal to the flow was used. The Reynolds number based on momentum thickness studied was 17000.

Figure 1 shows a top view of the set-up. The first concern is the validation of the experiment. For this topic, the vortex generators were removed in order to measure a canonical turbulent boundary layer. The PIV system was imaged with two Stereoscopic PIV systems in order to enlarge the field of view. Each system is based on Hamamatsu 2kx2k pixel cameras and micro Nikkor 105 mm lenses at $f\# 5.6$. The field of view of each system is about $40 \times 25 \text{ cm}^2$. Both systems were adjusted with a large overlap region in order to obtain, after merging, a final field of view of about $75 \times 28 \text{ cm}^2$. These dimensions are comparable to the boundary layer thickness in the wall normal direction and to about 5 integral scales in the spanwise direction. In that plane, the grid spacing is 2 mm which corresponds to 40 wall units.

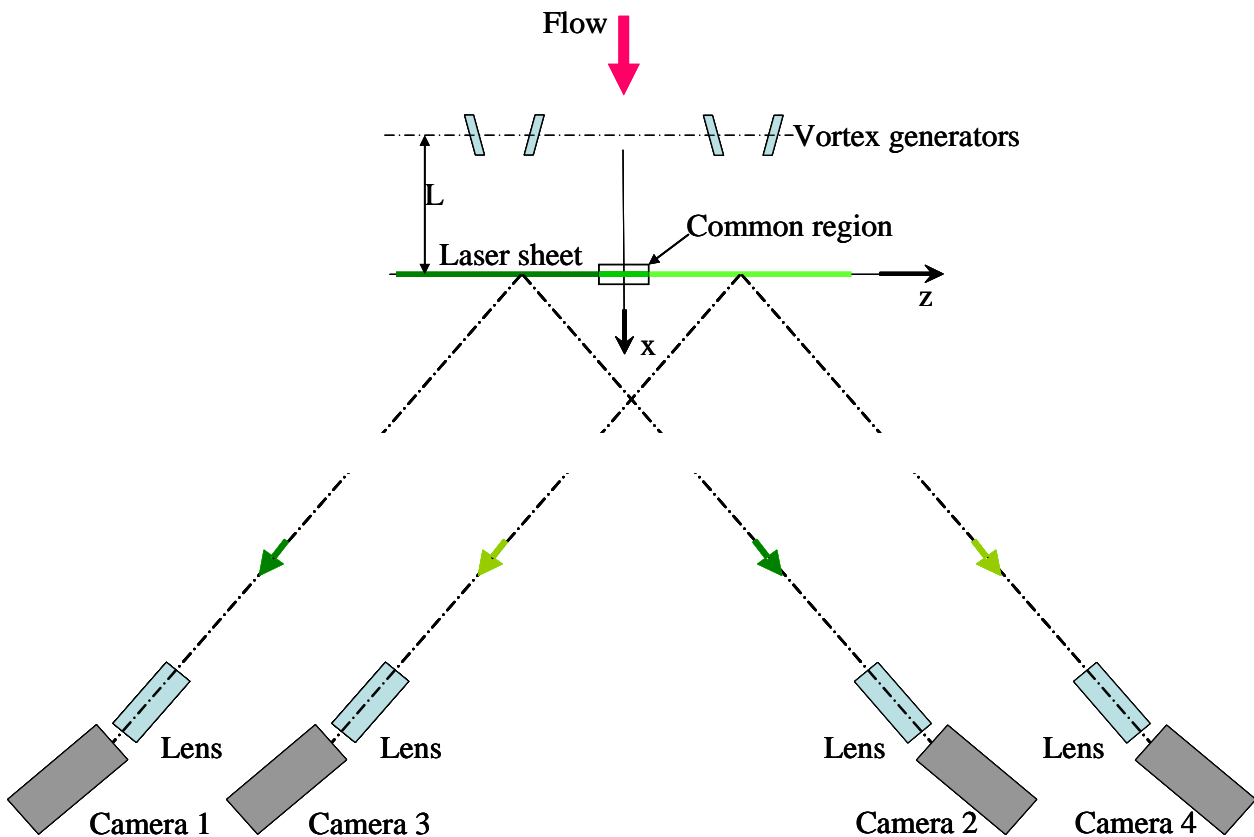


Figure 1 Experimental set-up

The laser used was a BMI YAG system with 2 cavities which is able to produce energy of 220 mJ per pulse at a frequency of 12 Hz. A mirror was stuck under the bottom glass in order to reflect the light in the wind tunnel and increase the light intensity. The beam waist was then located at the wall. Moreover each SPIV system was adjusted with respect to the Scheimpflug conditions (Willert (1997)). The seeding was Poly- Ethylene Glycol micron particles.

As explained in the first paragraph, the two light sheets were slightly separated in the streamwise direction, in order to optimize the dynamic range of the PIV. The separation is given by the mean velocity in the field

$$\Delta x = U \Delta t \quad (1)$$

of the order of 1.25mm (for an estimated mean velocity) with a light sheet thickness of about 1 mm (more than $6 u_{RMS}$) which allows a certain flexibility of the dynamics. Based on previous results obtained by hot wire anemometry, the local value of Δx can be estimated. Figure 2 gives the evolution of $\pm\Delta x/2$ given by the symbols with a range of $\pm 3 u_{RMS} \Delta t$ as a function of the wall distance. The two light sheets are also plotted in figure 2 respectively in green for the first and in red for the second pulse. The PIV delay is 250 μs in order to optimize the dynamic range with a minimum of filtering and a maximum of displacement. The maximal mean displacement is then 10 px with a RMS of 0.8 px close to the wall. Only for comparison figure 3 proposes the same result without separation of the light sheet, the thickness is kept at 1 mm. The optimized dynamic range has to be divided by 5 (maximum of displacement 2 px). From figures 2 and 3 the percent of paired particle images (deduced from a useful volume) can be estimated. Figure 4 shows the comparison of this number as a function of the wall distance. It is clear that the separated light sheet give a number of paired particle images double than the superimposed case. Figure 2 shows also that it could be very interesting to have a light sheet thickness which decreases when the wall distance increases in order to optimize the number of paired particles.

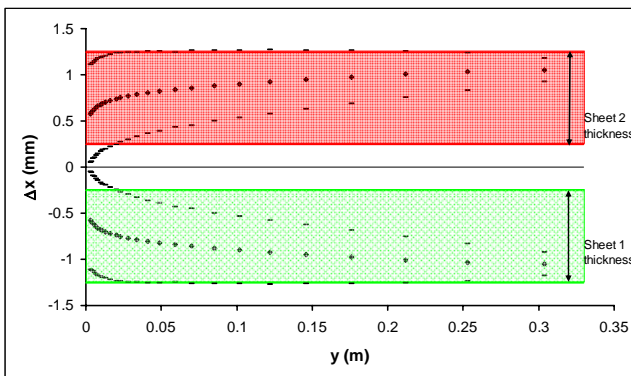


Figure 2 Light sheet separation scheme

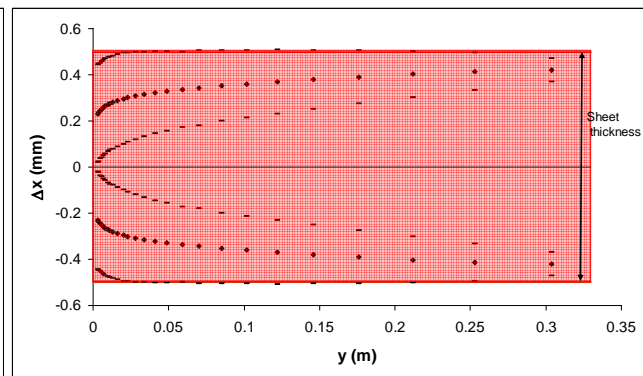


Figure 3 Light sheet superimposition scheme

In the present experiment, the self-correction process for each light pulse and for each SPIV system can be applied (Coudert and Schon (2001)). From the disparity map the location of each light sheet can be estimated. Figure 5 gives this location, in red and blue the two light sheets, in green the mean location. The distance between the two light sheets is about 1.2 mm as expected. A good continuity is clearly visible between the two SPIV systems (squares for the left system and diamonds for the right system). An angle of 0.15° between the light sheet and the calibration plane is also notable in figure 5. This angle can be easily compensated by the self-correction process. For the stereoscopic reconstruction, the Soloff method was used (Soloff et al (1997)). The calibration was done using 3 planes located at 0 and ± 2 mm giving a calibrated volume of 4 mm. The calibration volume is then of 4 mm per 750 mm which is larger than the illuminated particles.

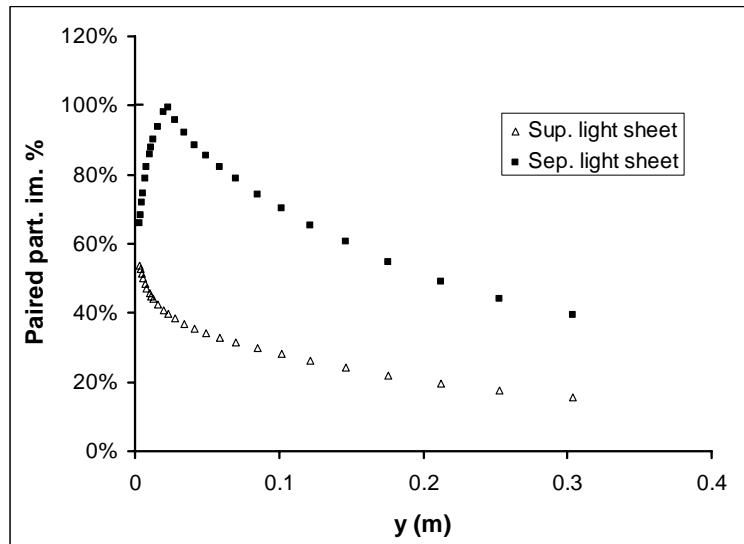


Figure 4 Estimation of the percentage of paired particle images square symbol for separated and triangle for superimposed light sheets

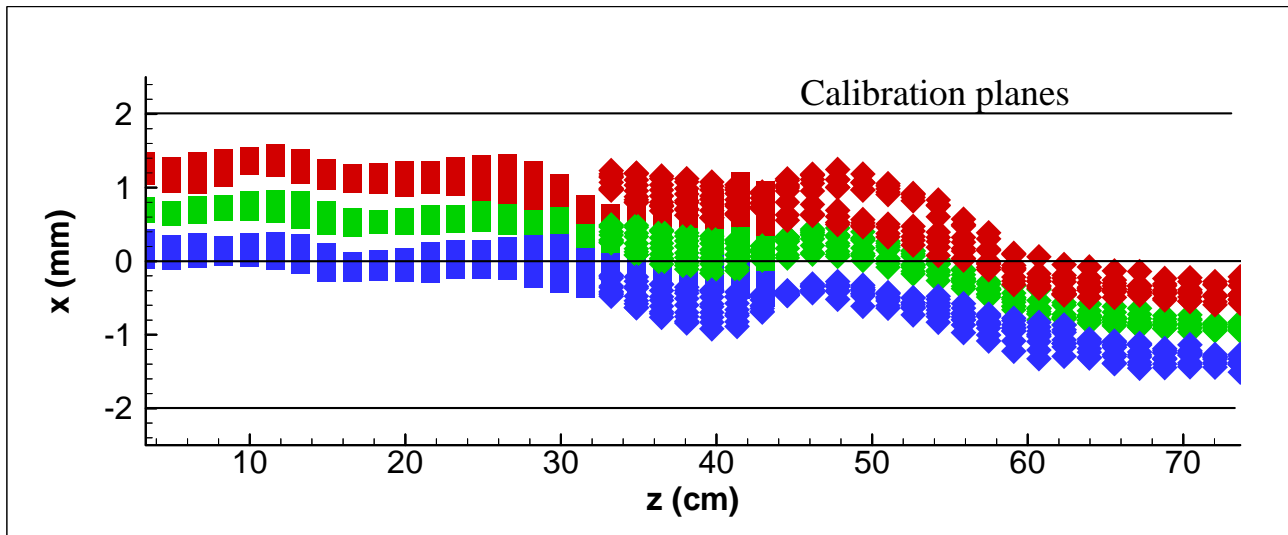


Figure 5 Relative locations of the light sheets deduced from the self-calibration process: first exposure (red), second exposure (blue), average light sheet location (green).

3. Accuracy

As explained previously, the first experiment was done without any vortex generator with the goal of validation and accuracy characterization. The large size (12 cm) of the overlap region allows us to study the accuracy of the PIV measurement. In this region, the estimated velocity is the averaged velocity for each component and the RMS error can be estimated:

$$\sigma_u(y) = \text{RMS}(u^1(y, z) - u^2(y, z)) \quad (2)$$

where u^1 and u^2 are the two measured velocities in the merge region. The RMS is computed over all samples (5000) and along z which is a homogeneous direction. The PIV processing was done using 3 passes with decreasing window sizes. Figure 6 gives the error for each component computed for 3 final window sizes: 18 x 24 px, 24 x 32 px and 32 x 48 px corresponding respectively to a square window of about 3.5 mm, 5 mm and 6.5 mm side (and about 70, 100, 130 wall units). The errors for the two stretched component u and w (figure (a) and (c)) are of the order of 2.5 % of the external

velocity U_e (corresponding to about 0.2 px) and increase when the wall distance decreases. They can reach 13 % close to the wall. This increasing is due to the mean velocity gradient (Foucaut et al (2003)). The error level far from the wall varies with the invert of the window size according to Foucaut et al (2004). This level for the v component (figure (b)) is smaller, it is of the order of 1.8 % which corresponds to almost $\sqrt{2}\sigma_u$ (clearly linked to the stereoscopic angle of 45°). The final choice was 24×32 px which gives a good compromise between accuracy and spatial resolution. The grid spacing of 2 mm leads to an overlapping of 60%.

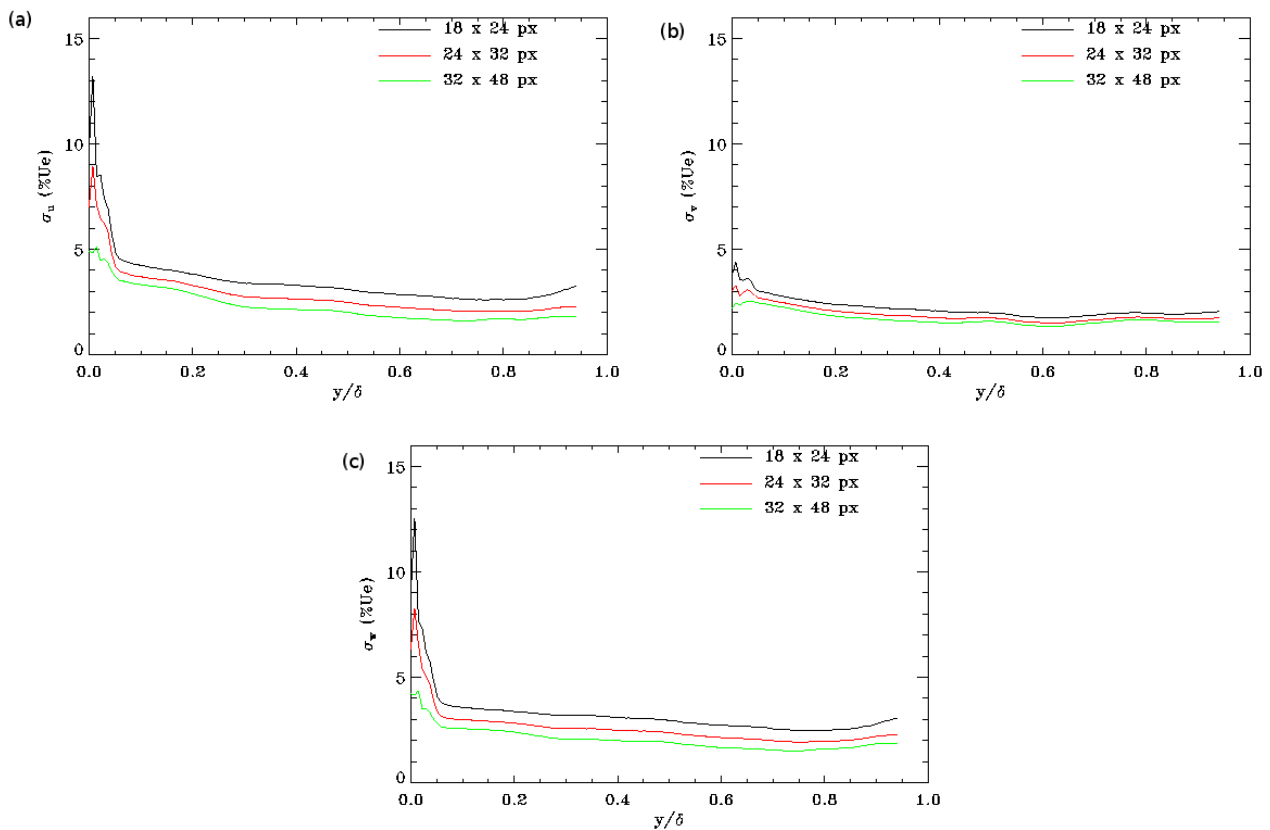


Figure 6 Estimation of the accuracy of each component.

To validate the results, statistics are computed by averaging along z and for all samples. Figure 7 shows a comparison between the mean velocity profile (left) and the turbulence intensity (right) measured by SPIV (blue) and hot wire anemometry (black symbols). Even if the Reynolds number is a little different (17000 for SPIV and 20800 for HWA) the agreement for the mean velocity profile is very good. There are few differences for the turbulence intensity profiles but they are in the range of error, a bar corresponding to 0.1 pixel is also plotted in this figure. This error is smaller for the standard deviation of the v component according to the accuracy estimation.

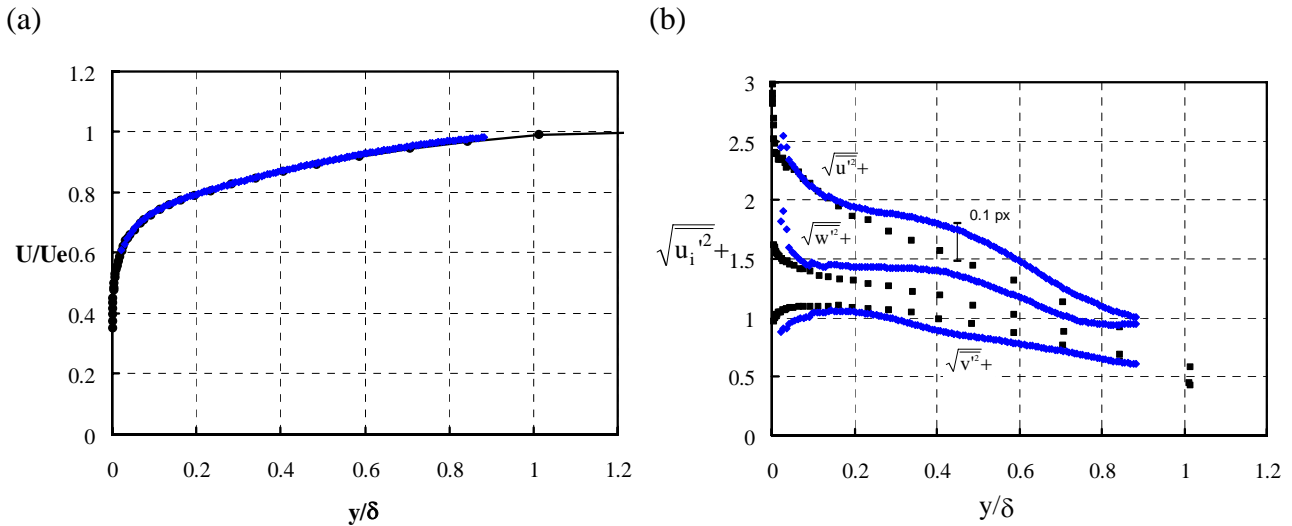


Figure 7 Statistical results without vortex generator (a) mean velocity profiles and (b) turbulence intensity

The vortex generators increase strongly the RMS value of the velocity in the first third of the boundary layer close to the wall. This increase induces a strong filtering of the velocity range which leads to large regions of spurious vectors in the heart of the vortices with the setup discussed previously. Consequently this led to a reduction of the PIV dynamic range and thus of the PIV delay in order to keep enough particles in the light sheet without too much filtering. In this case the PIV delay was $75 \mu\text{s}$ and the distance between the two light sheets was about 0.75 mm . The maximal mean displacement becomes 3 px with a RMS of 0.8 px which is comparable to the reference case. Figure 8 compares the error estimation without (a) and with (b) vortex generators located at $L = 2 \delta$ upstream the light sheet. Figure (b) shows an increase of these errors of about 60% for u and w and 20% for v . These errors correspond to about 0.15 px for u and w and 0.1 for v . The error variation is due to the lower dynamics.

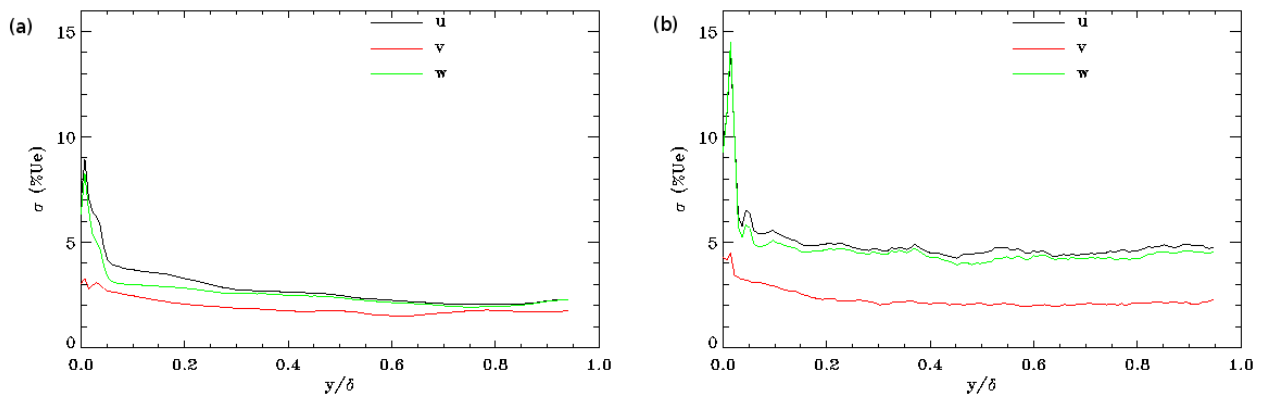


Figure 8 Estimation of the accuracy of each component with vortex generator located upstream the light sheet at $L = 2 \delta$.

Figure 9 gives for example a 3 components velocity field with vortex generators. The vectors correspond to the instantaneous in plane velocity components and the contour to the instantaneous streamwise (out of plane) velocity component. Two pairs of contra-rotating vortex are clearly visible.

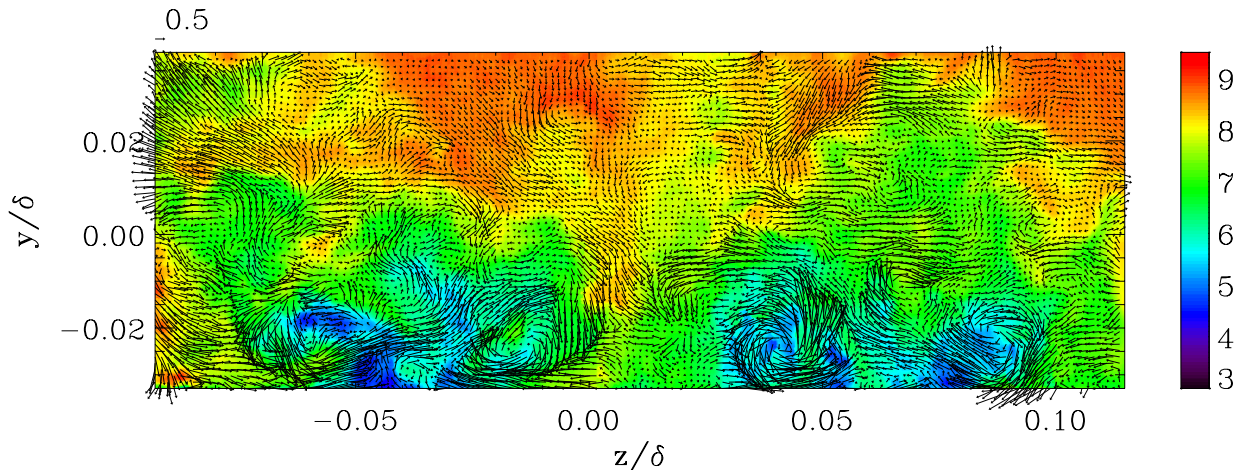


Figure 9 Example of 3 component velocity field with vortex generators.

3. Conclusions

The present paper gives guidelines to measure accurately the physics of vortices embedded in a turbulent boundary layer when the stereoscopic PIV planes are normal to the flow. The utility of a sheet separation in order to improve the measurement quality is discussed. It is shown how separation allows an optimization of the PIV dynamic range. It is demonstrating that the mean velocity and the fluctuation level have to be taken into account to adjust the experimental setup. Further, the accuracy is determined using the overlapping region of a double SPIV system.

The experiment is validated, its analysis is still in process and a database with several configurations of vortex generators is in preparation.

The outlooks are to characterize the physics of the streamwise vortices produced from vortex generators taking advantage of large scales of the turbulent boundary layer.

Acknowledgement

The work was supported through the International Campus on Safety and Inter modality in Transportation (CISIT) and the French Embassy grant N° 34/2011-CSU 8.2.1 as well as EUDP-2009-II-grant Journal number 64009-0279.

References :

- Adrian R.J. (1991) Particle-imaging techniques for experimental fluid mechanics, *Ann. Rev. Fluid Mech.*, 23, 261-304
- Carlier J. & Stanislas M. (2005) Experimental study of eddy structures in a turbulent boundary layer using particle image velocimetry. *J Fluid Mech*, 535, 143–188
- Coudert S. and Schon J. P. (2001) Back_projection algorithm with misalignment corrections for 2D3C Stereoscopic PIV, *Meas.Sci.Technol* 12, 1371-1381.
- Foucaut J.M., Carlier J., Stanislas M. (2004) PIV optimization for the study of turbulent flow using spectral analysis. *Meas Sci Technol* 15:1046–1058.
- Foucaut J.M., Miliat B., Perenne N. and Stanislas M. (2003), Characterization of different PIV algorithms using the EUROPIV Synthetic Image Generator and real images from a turbulent boundary layer, *EUROPIV2(book)*.

- Gad-El-Hak. (2000) M. Flow Control : passive, active and reactive flow management. Cambridge University press, ISBN 0 521 77006 8.
- Prasad A. K. (2000) Stereoscopic Particle Image Velocimetry, Exp. Fluids Suppl.:29, 103-116
- Soloff S., Adrian R. and Liu Z-C. (1997) Distortion compensation for generalized stereoscopic particle image velocimetry, Meas.Sci.Technol 8 (1997) 1441-1454.
- Westerweel J. (1997) Fundamentals of digital particle image velocimetry, Measurement Sc. and Tech., 8, 12, 1379-1392.
- Willert, C. (1997) Stereoscopic digital particle image velocimetry for applications in wind tunnel flows, Meas. Sci. Technol., 8, pp. 1465-1479.